JGR Atmospheres

RESEARCH ARTICLE
10.1029/2018JD029537

Key Points:
- The likelihood of rainy season onset occurring earlier than normal decreases as the local deforestation fraction increases
- The probability of occurrence of dry spells of any duration in this region is higher in areas with greater deforestation
- The delayed rainy season onset and longer dry spell events increase the climate risk to agriculture in the region

Correspondence to:
A. T. Leite-Filho,
argemirotlf@gmail.com

Citation:
Leite-Filho, A. T., de Sousa Pontes, V. Y., & Costa, M. H. (2019). Effects of deforestation on the onset of the rainy season and the duration of dry spells in southern Amazonia. *Journal of Geophysical Research: Atmospheres*, *124*, 5268–5281. https://doi.org/10.1029/2018JD029537

Received 23 AUG 2018
Accepted 9 APR 2019
Accepted article online 21 APR 2019
Published online 25 MAY 2019

Effects of Deforestation on the Onset of the Rainy Season and the Duration of Dry Spells in Southern Amazonia

Argemiro Teixeira Leite-Filho[1], Verônica Yameê de Sousa Pontes[1], and Marcos Heil Costa[1]

[1]Department of Agricultural Engineering, Federal University of Viçosa, Viçosa, Brazil

Abstract Amazonian deforestation is causing notable changes in the hydrological cycle by altering important precipitation characteristics. This study uses daily rainfall time series data from 112 rain gauges and a recent yearly 1-km land use data set covering the period from 1974 to 2012 to evaluate the effects of the extent of deforestation at different spatial scales on the onset of the rainy season and on the duration of dry spells in southern Amazonia. Correlation analyses indicate a delay in the onset of 0.12–0.17 days per percent increase in deforestation. Analysis of cumulative probability density functions emphasizes that the likelihood of rainy season onset occurring earlier than normal decreases as the local deforestation fraction increases. In addition, the probability of occurrence of dry spells in the early and late rainy season is higher in areas with greater deforestation. The delayed onset and longer dry spell events in highly deforested areas increase the climate risk to agriculture in the region.

1. Introduction

The Brazilian economic model of land use and exploitation of natural resources, characterized by the expansion of agricultural lands, predatory exploitation of timber, and accelerated urbanization, has caused great devastation to the Amazon biome, beginning around the end of the 1970s and continuing to the present.

Deforestation modifies some land surface properties that can affect both the amount and the partitioning of available energy on the surface. Forest removal increases the surface albedo and reduces the available net surface radiation. Furthermore, deforestation changes the partitioning of net radiation into latent and sensible heat flux by reducing surface roughness, leaf area index, and root depth. When compared to forested sites, deforested areas have higher albedo (18% compared to 13%; Culf et al., 1996), lower soil moisture storage capacity (because grasses have shallow root systems), and drier soils, all of which contribute to decreasing the latent heat flux. Cleared land may have a latent heat flux 30% lower than that of forested land (Gash & Nobre, 1997), and this means that stronger moisture transport and deeper convection are needed to trigger rainfall. In addition, reduced surface roughness decreases atmospheric turbulence and weakens vertical motion (Khanna & Medvigy, 2014).

In a region where precipitation is mainly convective (Marengo, 1995a, 1995b), these changes in land-atmosphere interaction may have caused important modifications in the regional hydroclimate, interfering in the hydrological cycle and altering important precipitation characteristics. Using 16 historical time series of precipitation for the state of Rondônia collected between 1961 and 2008, Butt et al. (2011) demonstrated that current trends in the delay in rainy season onset may be as great as 0.6 days/year, and after 30 years of deforestation, the onset was estimated to be 18 days later on average than it was before deforestation. Debortoli et al. (2015) also found delayed onset of the southern Amazon rainy season in more than 88% of the 200 rain gauges analyzed in the 1971–2010 period.

In addition to pointing out changes in precipitation timing, recent studies indicate that different hydroclimatic changes may be caused by different spatial scales of deforestation. Studying the onset of the rainy season, Debortoli et al. (2016) showed that rainfall seasonality is not correlated with forest cover at the microscale (1–15 km) but significant correlations appear at the mesoscale (30–50 km). This suggests that mesoscale atmospheric processes influenced by the land surface may have a greater influence on the onset of the rainy season.

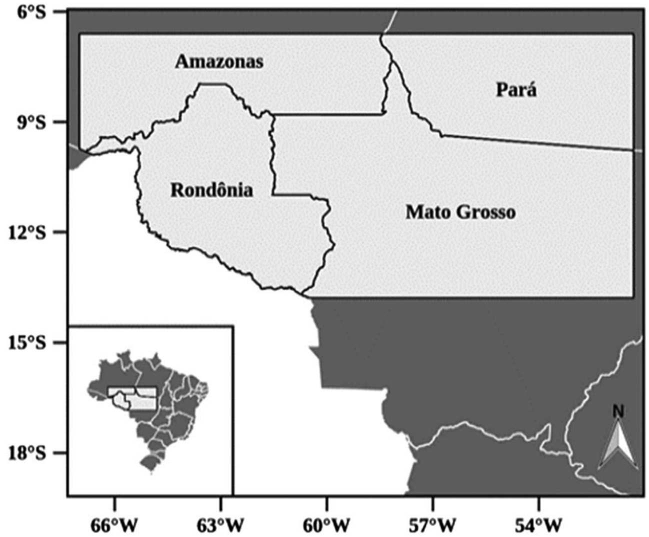

Figure 1. Location of study region within Brazil.

More recently, Khanna et al. (2017) explored controls on dry-to-wet season precipitation in Rondônia in southern Amazonia, concluding that changes in land cover affect the atmospheric circulation at the mesoscale, with rainfall typically decreasing over deforested areas. Chambers and Artaxo (2017), commenting on the results obtained by Khanna et al. (2017), raised the hypothesis that this shift in surface roughness would modify forest-atmosphere interactions, suggesting that deforestation is sufficiently advanced to have caused a shift from a thermally driven to a dynamically driven climatic regime.

Wright et al. (2017) described an important physical process for understanding how deforestation affects the southern Amazon rainy season using different remote sensing products. They showed that the interactions among land surface processes, atmospheric convection, and biomass burning can modify the timing of rainy season onset. These interactions precondition the atmosphere for regional-scale deep convection, which then leads to moisture convergence and consequently a rainy season onset two to three months before the southward displacement of the Intertropical Convergence Zone over the region. These studies, however, either considered only qualitative information on land cover or when they did consider quantitative land cover data, were fixed in time. Although this is not a problem for studies of a single season or for modeling studies, this is a significant limitation for hydroclimatic studies that analyze several rainy seasons in this region with intense land cover dynamics. A new yearly land cover and land use data set at 1-km resolution (Dias et al., 2016) now allow the exploration of explicit relationships between rainy season characteristics and deforestation extent.

Other studies have investigated the occurrence of dry spell events in several regions of Brazil and the large-scale climatic variations associated with them (Assad et al., 1993; Carvalho et al., 2000; Minuzzi et al., 2005; Silva & Rao, 2002; Sleiman, 2008). However, Erfanian et al. (2017) argued that recent dry periods in the Amazon cannot be explained only by changes in sea surface temperature, suggesting that other factors are contributing to severe drought. Here we also investigate the relationship between deforestation and dry spells in the region.

This study has two main goals. First, we revisit the relationship between rainy season onset and the scale of deforestation in southern Amazonia using the yearly land use data of Dias et al. (2016). Second, we evaluate the relationship between the scale of deforestation and the duration of dry spells occurring during the rainy season (September to April). Both analyses provide relevant information to the local agricultural sector.

2. Data and Methods

2.1. Region Studied

The area studied is southern Amazonia, which ranges from 6 to 14°S latitude and from 65 to 51°W longitude and includes the state of Rondônia, southern Amazonas, northern Mato Grosso, and southwestern Pará (Figure 1). This region was selected because it possesses five characteristics fundamental for the study: (1) rain that is typically convective (Marengo, 1995a, 1995b); (2) strong coupling between forest and climate (Fu et al., 2013); (3) strong rainfall seasonality, with well-defined dry and rainy seasons (Davidson et al., 2012; Marengo, 2004); (4) considerable albedo differences between native vegetation and deforested areas (Culf et al., 1996); and (5) intense deforestation in the past several decades (Dias et al., 2016). These characteristics are expected to facilitate the detection of a relationship between deforestation and the rainy season.

Containing the major part of the arc-of-deforestation (Ferreira et al., 2005), this region has been the center of major and rapid deforestation activities in the Brazilian Amazon since the 1970s, having areas with a large range of spatial scales of deforestation. Changes in land cover from 1970 to 2012 within the study area affected 191,319 km^2 (Dias et al., 2016), or 48.2%, of the total deforestation by 2012 in the Amazon (396,850 km^2; Instituto Nacional De Pesquisas Espaciais, 2012).

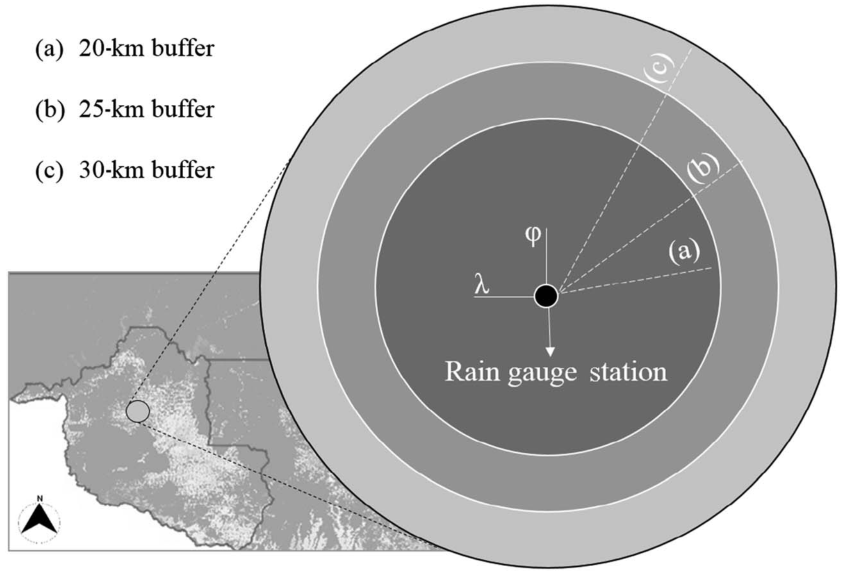

Figure 2. Illustration of the applied methodology showing an example of three buffer zones of differing radii surrounding a single rain gauge station: (a) 20, (b) 25, and (c) 30 km. The percentage of deforested land in each of these zones was analyzed in relation to the associated rain gauge data. Rain gauge station locations are identified by latitude (φ) and longitude (λ).

The historical causes of deforestation in this region include predatory exploitation of forests for timber (Nepstad et al., 2001) and infrastructure expansion, such as road building and urbanization (Carvalho et al., 2001; Laurance et al., 2001). Later, expansion of cropland (especially soybeans) and pastureland became major driving forces (Dias et al., 2016; Macedo et al., 2012; Morton et al., 2006).

2.2. Land Cover Data

We used the land use database developed by Dias et al., 2016 as our main source of land cover data. This historical reconstruction provides the longest agricultural land cover and land use database currently available for this region. These data were produced from a combination of yearly remote sensing data (Hansen et al., 2013), which provided the locations of forest cover, and agricultural census data, which provided the link between deforested areas and agricultural land use. The results were then aggregated at 30″ spatial resolution (approximately 1×1 km). The final data are in hectares per pixel, which for our analysis were converted into percentages of deforested land per 1-km^2 pixel.

We calculated the ratio of deforested area within different spatial scales based on the concept of buffer zones, similar to Debortoli et al. (2015). This approach consists of using three circular buffer zones centered on the coordinates of each rain gauge station, with radii equal to 20, 25, and 30 km (Figure 2). Defining buffer zones of fixed sizes allowed the calculation of the deforestation fractions in each year and the calculation of correlations between specific rainy season properties and deforestation fractions at different scales.

2.3. Rainfall Data

We analyzed daily rainfall data from 112 stations across the region, covering the period from 1974 to 2012, which we obtained from the Hydrological Information System of ANA (Brazil's National Water Agency; *HidroWeb*, http://hidroweb.ana.gov.br/, accessed 2016, Figure 1). Of these time series, 60 cover more than 20 years and 15 cover more than 30 years (Appendix A and Table A1).

We performed quality control procedures on the rainfall data used in our analysis. For each rainfall station, we completely eliminated any years of the time series that met one or more of the following three criteria: (1) they included daily precipitation values greater than 350 mm (we considered these to be either measurement errors or rare extreme events that we eliminated from the analysis to avoid biases; Fetter et al., 2018); (2) they presented a sequence of equal daily rainfall values for seven or more days (e.g., exactly 10 mm every day for

9 days), indicating possible measurement errors; or (3) they included one or more missing data points between 1 September and the onset of the rainy season for that hydrological year.

2.4. Identification of Rainy Season Onset and Dry Spells

The rainy season (period of strong convective activity) in the Amazon comprises the months of November through March, and the dry period, May through September (Figueroa & Nobre, 1990; Marengo, 1995a, 1995b). In this study, to encompass the annual transition period between the dry season and the rainy season (September and October), the period of analysis begins in September of each year and ends in April of the following year.

Several methods have been developed to identify rainy season onset dates in tropical regions (Butt et al., 2011; Liebmann et al., 2007; Liebmann & Mechoso, 2011; Marengo et al., 2001; Odekunle & Buyiro, 2003; Stern & Coe, 1982; Sugahara, 1991). Stern and Coe (1982) defined rainy season onset as the first day on which precipitation is equal to or greater than 20 mm/day for two or three consecutive days if there is no period of seven or more days with zero precipitation in the following month. Oliveira (2000) adopted this method for estimating planting dates for rice in the Brazilian state of Minas Gerais with good agreement to observed dates. More recently, Butt et al. (2011) defined rainy season onset in the Brazilian state of Rondônia as the first day after 1 September (inclusive) when daily precipitation exceeds 20 mm.

Following Stern and Coe (1982), we defined rainy season onset ($B_{i,j,t}$, where B stands for *beginning*) as the first day after 1 September (inclusive) that has daily precipitation greater than 20 mm followed by at least one more rain event (daily precipitation more than 1 mm) in the subsequent 7-day period. The subscripts i, j, and t refer to latitude, longitude, and year, respectively. The dates were indexed so that 1 September becomes *Day 1*, 2 September is *Day 2*, and so on.

The definition of a dry spell ($DS_{i,j,t}$) varies among studies according to the objectives in each case (Sharma, 1996; Ceballos et al., 2004; Soares & Nóbregabrega, 2010). In this study, we defined $B_{i,j,t}$ and $DS_{i,j,t}$ based on agricultural criteria, since our interest relates to the importance of rain for rainfed agriculture in the region. A dry spell is an event characterized by a minimum of eight consecutive days with daily precipitation less than 1 mm and starting after $B_{i,j,t}$, as previously defined. This represents a drought interval potentially damaging to crops and is similar to the definition of Assad and Sano (1998).

The $DS_{i,j,t}$ duration is calculated in days and is classified according to the month in which a $DS_{i,j,t}$ event starts. For example, if a dry spell event begins on 28 September and ends on 13 October, the starting month is September. Next, we divided the rainy season into an early rainy season (SO, including the months of September and October, postonset), a peak rainy season (NDJF, including November, December, January, and February), and a late rainy season (MA, including March and April).

2.5. Anomalies in Rainy Season Onset

There is a precipitation seasonality gradient across the Amazon, and consequently, geographical position affects rainy season temporal parameters (Butt et al., 2011; Costa & Foley, 1997; Gan et al., 2004; Marengo et al., 2001; Sombroek, 2001). Therefore, we based our analyses on the anomalies of the $B_{i,j,t}$ values ($B'_{i,j,t}$), removing the signal of the geographic position and the interannual variability (which reflect the effects of large-scale mechanisms) to find evidence of the deforestation signal. To calculate these anomalies, first we estimated the parameters of the linear equation that describe the best fit linear regression relationship between $B_{i,j,t}$ and geographic coordinates (latitude [φ] and longitude [λ] specified in degrees rather). The resulting geographical trend is explained by Equation (1),

$$\widehat{B}_{i,j} = 30.44 - 0.97\varphi + 0.29\lambda \tag{1}$$

where negative values of latitude indicate locations south of the equator, and negative values of longitude refer to locations west of the Greenwich meridian. We then calculated the onset anomalies ($B'_{i,j,t}$) by subtracting the geographical trend and the annual averages (mean anomaly at all stations for a specific year, equation (2)):

$$B'_{i,j,t} = \left(B_{i,j,t} - \widehat{B}_{i,j}\right)_{i,j,t} - \overline{\left(B_{i,j,t} - \widehat{B_{i,j}}\right)}_{t} \tag{2}$$

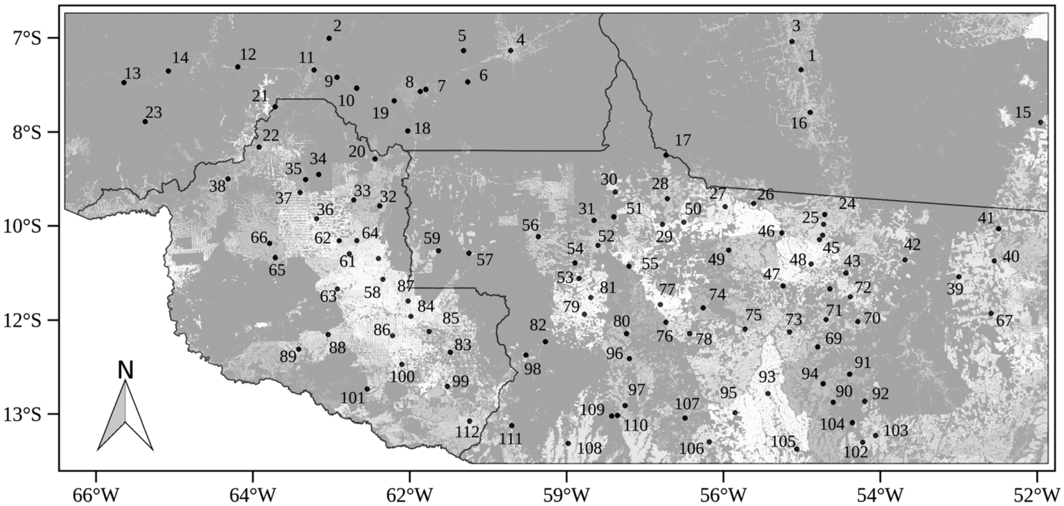

Figure 3. Distribution of rainfall stations in the region studied in relation to areas of deforestation in the year 2012. Light gray pixels represent areas deforested in 2012.

2.6. Data Analysis

Initially, to demonstrate the gradient of onset of the rainy season ($B_{i,j,t}$) across the entire study area, we constructed $B_{i,j,t}$ maps for 1985, 1995, and 2005. We interpolated $B_{i,j,t}$ data from rain gauge stations and estimated sample variograms. Next, we fitted $B_{i,j,t}$ with a Gaussian spherical model (Pebesma, 2004; Pebesma & Heuvelink, 2016).

To consider the correlation between deforestation and time, separating the effects of deforestation from the mean long-term trend in $B_{i,j,t}$, we performed t tests to compare the onset of the rainy season between stations without significant change in their deforestation fraction over time and stations that experienced increasing deforestation within the 25-km buffer. For this, we subsampled 20 stations spatially distributed in the region (Figure 3) that provided time series longer than 25 years and divided them into two groups (Table 1).

Next, we investigated the correlation between deforestation fraction and $B'_{i,j,t}$. For each buffer circle size, we classified the deforestation fraction into eight classes: Class 1 has < 5% of its area deforested; Class 2 has between 5% and 10% deforested; and so on, through Class 8, with between 35% and 40% deforested. We averaged $B'_{i,j,t}$ for each deforestation class and found that the means of onset anomalies $\left(\overline{B}'_{i,j,t}\right)\cdot B'_{i,j,t}$ were normally distributed (Shapiro-Wilk test, $p < 10^{-9}$, Shapiro & Wilk, 1965); thus, it was appropriate to apply a linear regression model and estimate the standard error of the mean.

To compare the effects of deforestation on the frequency of dry spells of any duration, we performed t tests against the null hypothesis that the mean duration of $DS_{i,j,t}$ is not significantly different between two deforestation classes (0%–20% and 20%–40%) for the 20- and 25-km buffers for three periods of the rainy season: SO, NDJF, and MA.

We assigned probabilities directly based on the $B'_{i,j,t}$ and $DS_{i,j,t}$ elements according to the probability of occurrence in the sample space generated. For this, we constructed cumulative probability density functions

Table 1
Selected Stations That Provided Time Series Longer Than 25 Years and Groups Divided by Deforestation Fraction in the 25-km Buffer Zones

Group	Stations	Mean latitude	Mean longitude	Period	Mean deforestation (%)
1	5, 6, 12, 13, 17, 35,			1970s–1980s	4.1
	36, 39, 83, 85	−9.1697	−60.5167	1990s–2000s	3.9
2	16, 20, 42, 46, 56,			1970s–1980s	4.2
	73, 77, 96, 102, 108	−10.4988	−56.8653	1990s–2000s	13.0

10.1029/2018JD029537

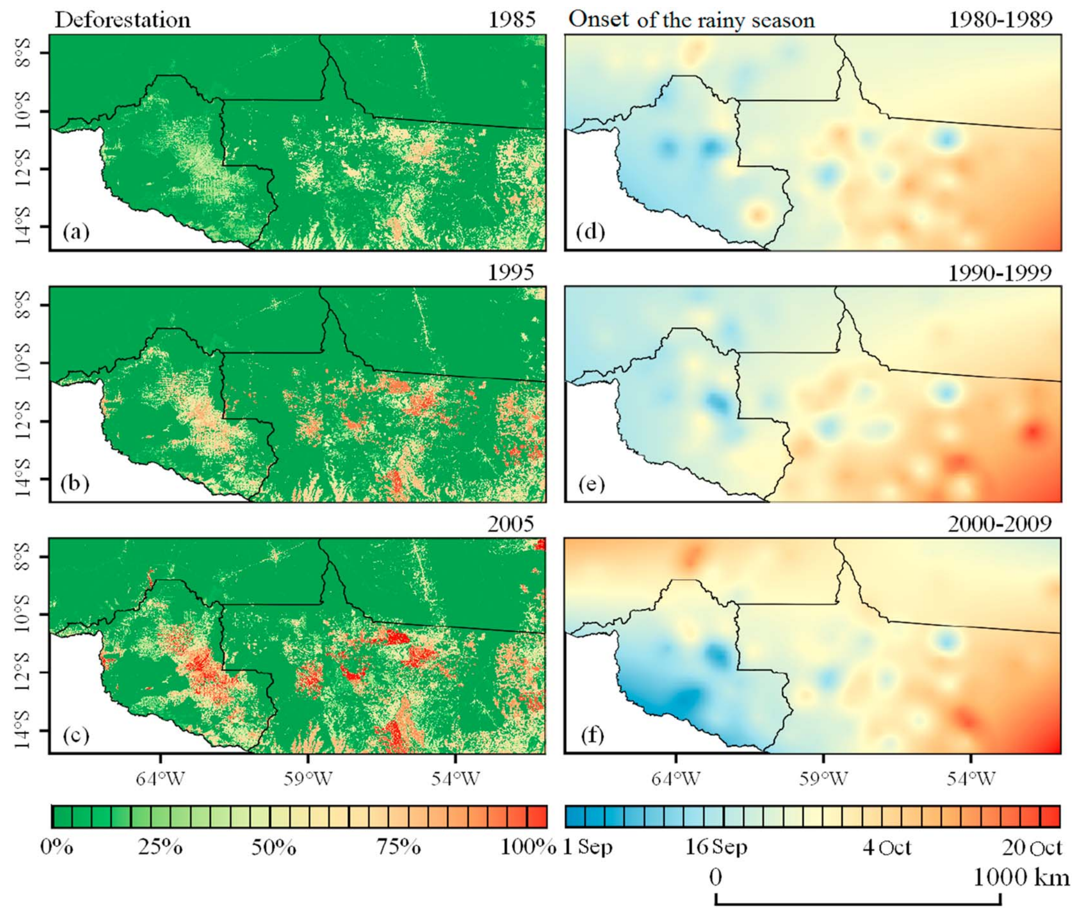

Figure 4. Evolution of deforestation in the region studied for (a) 1985, (b) 1995, and (c) 2005, and mean of rainy season onset dates for each of three decades: (d) 1980–1989, (e) 1990–1999, and (f) 2000–2009.

(CDFs) of $B'_{i,j,t}$ and $DS_{i,j,t}$ divided into two contrasting classes of deforestation (0–5% and 30–35%), which we considered to be low and high deforestation rates, respectively. The graph of the CDFs was generated as a product.

3. Results

The $B_{i,j,t}$ maps revealed a northwest-to-southeast gradient in the study area (Figures 4d–4f), which has also been found in other studies (Costa & Foley, 1997; Sombroek, 2001; Vilar et al., 2009). This gradient is due to the interactions between tropical convection systems and midlatitude frontal systems leading to the appearance of the South Atlantic Convergence Zone during springtime, indicating a gradual arrival of the rainy season (from NW to SE), and corresponding to a gradual onset of the South American monsoon (Gan et al., 2004). This result reinforces the importance of controlling for the influence of geographical position in the onset data.

Coincidentally, land use patterns have demonstrated a similar gradient (Figures 4a–4c), with areas in the north presenting more natural forest cover, corresponding to the historical occupation of Amazonia related by previous studies (Carvalho et al., 2001; Dias et al., 2016; Laurance et al., 2001; Morton et al., 2006; Nepstad et al., 2001).

Table 2 displays the average of $B_{i,j,t}$ in the 1970s–1980s as compared to the 1990s–2000s for two station groups and the results of the independent two-sample *t* test. For stations within areas with increasing deforestation fractions over the years (Group 2), $B_{i,j,t}$ was delayed by about 6 days, whereas for stations within areas with constant land cover (Group 1), the delay was about 2 days.

Table 2
Results of the Independent Two-Sample t Test With Unequal Sample Sizes and Unequal Variance of the Means of $B_{i,j,t}$ for Station Groups 1 and 2 for the 1970s–1980s and for the 1990s–2000s (μ1970s–1980s and μ1990s–2000s)

Group	$\mu_{1970s-1980s}$	$\mu_{1990s-2000s}$	$S^2_{1970s-1980s}$	$S^2_{1990s-2000s}$	t_{calc}	$P_{1\text{-tailed}}$
1	17 Sep	19 Sep	4.6	5.1	0.351	0.347
2	18 Sep	24 Sep	4.8	5.5	−2.133	0.011

The t test results indicate that for Group 2, the $B_{i,j,t}$ is significantly different between the 1970s–1980s and 1990s–2000s at the 98.9% confidence level. However, for Group 1 no significant difference in onset was found between the periods for the group with constant land cover.

Figure 5 shows the means of rainy season onset anomalies ($\overline{B}'_{i,j,t}$) in different deforestation classes after removing the effects related to geographical position and year, and it shows the corresponding values for standard error of the mean. The linear regressions for the 20-, 25-, and 30-km buffers evidence a delay in $B_{i,j,t}$ of 0.12–0.17 days per each 1% increase in deforestation. All the trends are significant at the 99% confidence level. Considering these coefficients, a deforestation rate of 50–60% corresponds to about a 1-week delay in the rainy season onset. The trends evidenced differences between the three buffer sizes.

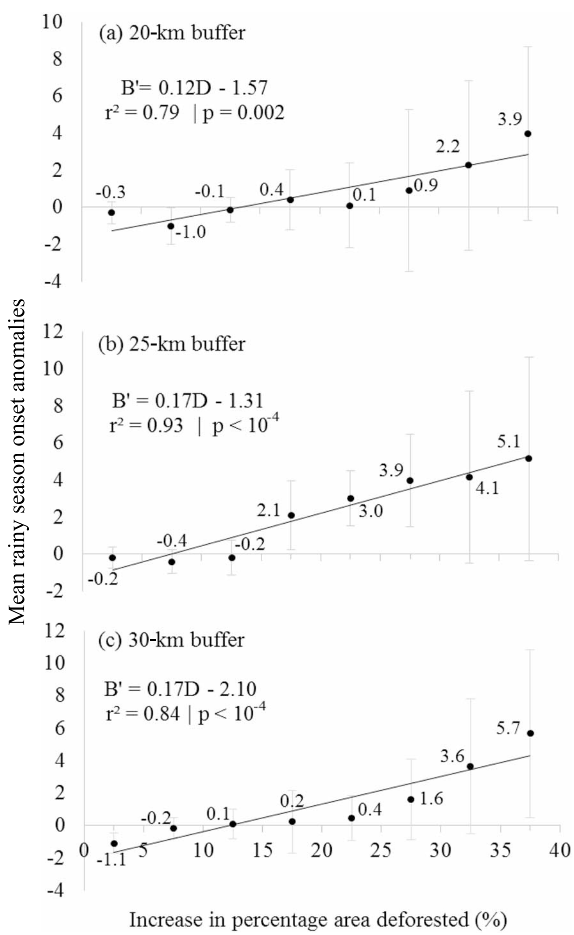

Figure 5. Mean of rainy season onset anomalies in different deforestation classes, and the standard error of the mean for the three buffer sizes: (a) 20, (b) 25, and (c) 30 km. Best fit linear regression line and associated parameters are also shown.

Although the average of onset anomalies is representative of each deforestation class, it is also possible to calculate the probability of occurrence of $B'_{i,j,t}$ using CDFs. Figure 6 shows that, for the buffers larger than 20 km, in years when the rainy season starts later, there is little difference in whether a region is heavily deforested or not; in this situation, the transition from the dry season to the rainy season is probably dominated by large-scale mechanisms (which were removed from the first part of our analysis, as described above). However, in years when the rainy season starts earlier, greater forest cover is associated with earlier $B_{i,j,t}$, since it increases the sensitivity of the system to large-scale mechanisms.

In addition to being able to anticipate rainy season onset dates, knowing the probability that a dry spell event ($DS_{i,j,t}$) will occur after the rainy season onset is also useful information for farmers in rainfed systems.

The t test results for $DS_{i,j,t}$ duration differences between the high and low deforestation classes for the periods of SO, NDJF, and MA (Table 3) indicate that for the SO and MA periods, for 25-km buffer sizes, the duration of dry spells was higher in the more deforested area at the 99% confidence level and slightly less significant for the 20-km buffer size (98% confidence level). However, for NDJF, there was no significant difference in $DS_{i,j,t}$ duration between the deforestation classes.

Figure 7 shows the CDFs of the duration of DS events lasting 8 days or longer, for 20- and 25-km buffer sizes, in two deforestation classes. For all the buffers analyzed, the probability of occurrence (an estimate of how often a DS of equal duration occurs) of longer DS events is higher in the areas that have experienced greater deforestation (of 30–35%, by area) than in the less deforested areas (0–5% deforested), regardless of the event's duration. We also observe a more evident contrast between the deforestation curves (0–5% and 30–35%) in SO and MA (early and late rainy season) as compared to NDJF (peak of the rainy season). The more evident differences during the early and late periods emphasize when deforestation appears to make a difference.

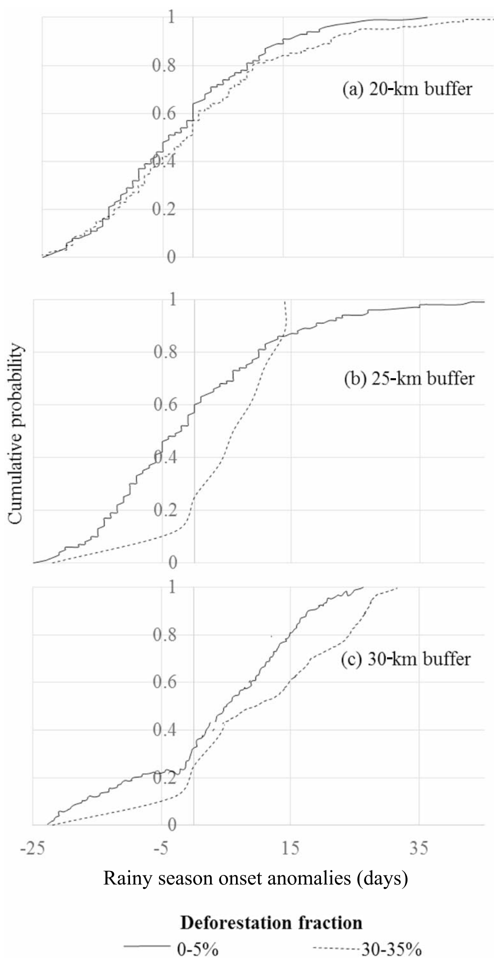

Figure 6. Cumulative probability density function (CDF) of the rainy season onset anomalies for three different buffer sizes: (a) 20, (b) 25, and (c) 30 km.

In SO, for the 25-km buffer, the probability of occurrence of a dry spell of ≥ 15 days in a region 0–5% deforested is about 23%, and this risk increases to about 55% in areas with deforestation between 30 and 35% (Figure 7b). For the same buffer size, in MA, increased deforestation also increases the probability of occurrence of a dry spell of the same duration (≥ 15 days). In areas with low deforestation, this probability is null, whereas in areas with high deforestation, the probability is 17% (Figure 7f).

Even if the CDFs for the peak wet season are not much different between the deforestation classes, the more evident differences during the early and late periods emphasize that during SO and MA, deforestation appears to have made a difference.

4. Discussion

Although methodological differences do not allow for direct quantitative comparison with some studies, the trend toward delayed onset of the rainy season as suggested by our linear regressions can also be found elsewhere in the literature (Butt et al., 2011; Costa & Pires, 2010; Debortoli et al., 2015; Debortoli et al., 2016). Butt et al. (2011) used a definition of onset very similar to the one used in this study, but they did not quantitatively analyze the effect of deforestation. They found delays of as much as 0.6 days/year in the state of Rondônia; this equates to 18 days over the 30 years of their analysis, during which about 22% of the state was deforested. It is possible that the reason the rainy season onset delay identified in our study is smaller than their result is because we controlled for most of the effects associated with trends in large-scale hydroclimate mechanisms, leaving only the deforestation effect. Of the 38 stations in our study with more than 25 years of data, 65% have exhibited delayed rainy season onset. Similarly, Debortoli et al. (2015) reported onset delay in 63% of the time series analyzed for the southern Amazon. The increase in deforestation impact with increased buffer size may be associated with different sizes of convective cells affecting deep cloud development over the buffers studied. The rain gauge data, however, are not sufficient for more solid conclusions on this matter, and high-resolution radar data would be required. Operational meteorological radars are unfortunately not available in this region.

In southern Amazonia, regional high humidity originating in the rain forest provides latent heat fluxes that promote convection. Deforestation affects energy partitioning, decreasing the latent heat flux and causing a drier-than-usual atmosphere, thus delaying the onset of the rainy season (Schubert et al.,

Table 3
Results of the Independent Two-Sample t Test With Unequal Sample Sizes and Unequal Variance of the Means of DS Duration (μ_1 and μ_2) for Deforestation Classes 1 (0–20%) and 2 (20–40%)

Buffer size	Period	μ_1	μ_2	n_1	n_2	$S_?^2$	$S_?^2$	t_{calc}	$P_{1\text{-tailed}}$
20 km	SO	13.0	15.2	2258	1078	40.1	38.5	−2.0431	0.011
20 km	NDJF	11.5	10.9	947	1582	21.9	6.3	0.348	0.362
20 km	MA	13.6	14.9	2154	1586	42.7	63.1	−2.0442	0.012
25 km	SO	13.3	14.4	2193	201	7.4	8.6	−2.5945	0.003
25 km	NDJF	9.6	9.8	736	356	8.6	9.8	0.2461	0.250
25 km	MA	12.8	14.8	1945	710	22.9	9.5	−2.5847	0.008

Note. NDJF = November, December, January, and February; SO = September and October; MA = March and April.

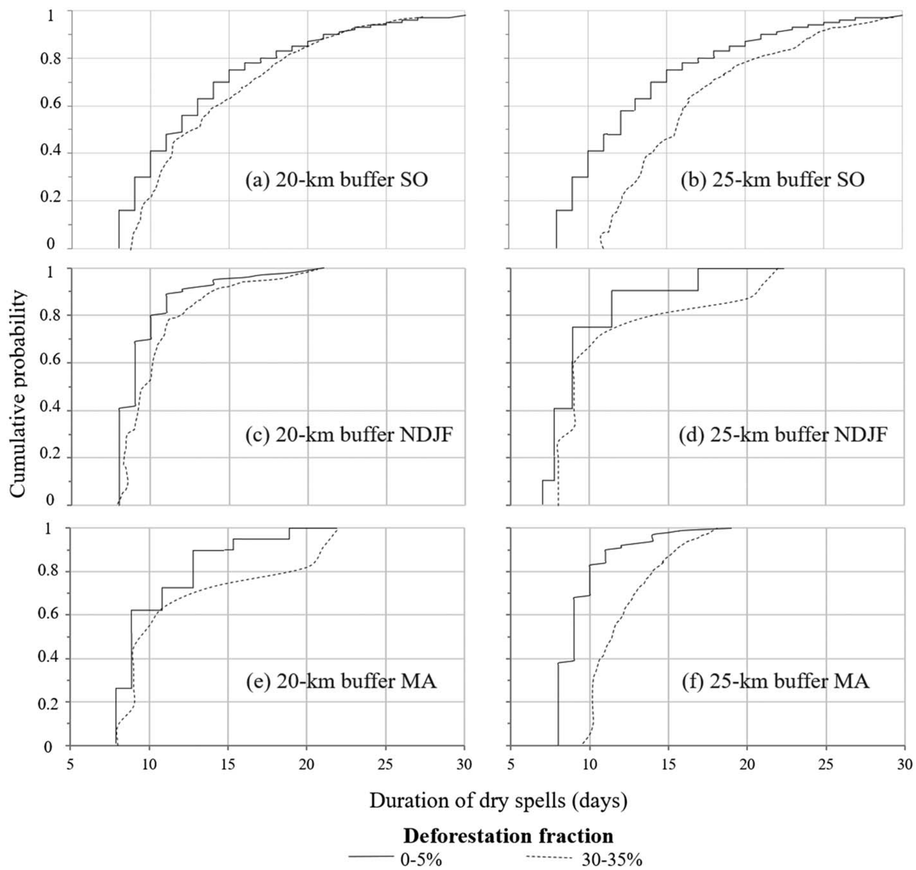

Figure 7. Cumulative probability density function (CDF) of the duration of dry spells for the early rainy season (SO, postonset), for the peak rainy season (NDJF), and for the late rainy season (MA) for two different buffer sizes: (a) 20 km, SO; (b) 20 km, NDJF; (c) 20 km, MA; (d) 25 km, SO; (e) 20 km, NDJF, and (d) 25 km, MA. NDJF = November, December, January, and February; SO = September and October; MA = March and April.

2004). These results are also consistent with the shallow convection moisture pump mechanism proposed by Wright et al. (2017). At the scale of the buffers studied (mesoscale), complete or partial clearance of forest affects transpiration and weakens the conditions that promote surface convection, moistening, and destabilizing the atmosphere, until finally causing a delay in the onset of the rainy season.

In some cases, especially in drought years, delays of these magnitudes in rainy season onset could jeopardize double-cropping systems as deforestation at these levels spreads (Abrahão & Costa, 2018; Spangler et al., 2017). For double-cropping systems (here typically soybean followed by corn) to be viable, farmers need to ensure that the soybeans are harvested in time for the second crop to mature while climatic conditions are still favorable. Delays in rainy season onset may lead to a reduction of areas and years where double-cropping systems will be feasible with low climate risk.

In addition, the higher probability of longer DS events in areas that are more heavily deforested may lead to water deficit and have consequent negative effects on agricultural production, depending on the cultivar and its stage of development. This relationship between DS events and agricultural problems has already been widely investigated (Carvalho et al., 2000; Barron et al., 2003; Silva & Rao, 2002; Soares & E Nóbrega, 2010; Adekalu et al., 2009; Barron & Okwach, 2005; Fox & Rockström, 2003; Hernandez et al., 2003; McHugh et al., 2007).

Water deficit has a direct effect on final crop production, which depends on the crop and its stage of development (Doorenbos & Kassam, 1979). This has been demonstrated in studies such as Espinoza et al. (1980), which showed reductions of up to 60% in maize yield when dry spells occurred between the flowering stage and the grain-filling stage, and Espinoza et al. (1982), which found yields for irrigated soybean higher by 24% to 55% compared to crops experiencing water deficiency.

Occurrence of longer DS events (more likely to occur in more deforested areas) during the period of crop growth is a serious risk to agricultural production, since, as plants develop, the need for water increases and reaches maximum demand during flowering and grain-filling stages, after which the need decreases. Many consecutive dry days could exacerbate soil moisture deficits, interrupting consistent resupply of soil moisture to crops, affecting the amount of water available to the plants, and reducing agricultural yields (Doorenbos & Kassam, 1979).

In particular, we find that differences in dry spell CDFs between the two deforestation classes are only significant in SO, when the rainy season typically begins, and MA, when the rainy season typically ends. These results may be sensitive to the definition of rainy season onset used. Short-lived rain events caused by the passage of cold fronts or other synoptic-scale systems may confound the identification of the rainy season onset. Similarly, the differences in MA might imply earlier, more abrupt end of the rainy season over deforested regions.

This analysis has direct applications to agricultural planning and decision making. In terms of risk to agriculture due to weather conditions, if farmers choose to plant a single crop based on the presented results, they will benefit from waiting for a more secure scenario to start sowing the crop. The secure scenario is one that minimizes the probability of being affected by either delay in the onset of the rainy season or occurrence of extreme weather phenomena, such as dry spells of higher durations. A good choice of sowing season tries to match the needs of the crop during all of its developmental stages with times when favorable climatic conditions are most likely. In the case of soybeans, the sowing time should coincide with the period of the year when the water stored in the soil is most likely to be found in sufficient quantity for seed germination and seedling emergence, and therefore the establishment of the field crop; this sowing window may happen earlier in less deforested sites. These inferences are generic for the region; for farms that are located farther north in the study region, the rainy season is expected to start a few days sooner than in the southernmost part of the region.

5. Conclusions

This research disentangles the complicated relationship between deforestation and precipitation in southern Amazonia. By removing regional trends and interannual variability, our results demonstrate that increased deforestation contributes to delayed onset of the rainy season. For all scales analyzed, correlation analysis shows increasingly delayed rainy season onset through time as deforestation progresses. Analysis of cumulative probability density functions for rainy season onset indicates that in years that the rainy season starts earlier, the absence of forest cover delays the onset of the rainy season. In addition, a higher percentage of deforestation is also associated with a higher frequency of long dry spell events during the early and late rainy season as compared to minimally deforested regions. Land use changes happening in the study area may be imposing strong physical changes that affect the amount of potential energy available for moist convection. These changes are due to latent heat and albedo alteration occurring in response to surface changes and have, in turn, been influencing rainy season duration (Dubreuil et al., 2012; Fu et al., 1999, 2013).

The increased deforestation also increases climate-related risks to agriculture in southern Amazonia. Specifically, considering the double-cropping system practiced in the region, a delay in the onset of the rainy season may limit the feasibility of growing two successive crops. It is also important for the selection of cultivars to be planted by farmers in rainfed systems, since cultivars characterized by a long juvenile period and cultivars of medium and late maturation poorly tolerate late sowing due to delayed onset of the rainy season or longer dry spell events—events that we have demonstrated are more likely to occur in areas of greater deforestation. In addition to providing information to support crop management and planning, such information is also a tool with great potential for analysis by the insurance market, and it may also be important for the development of regional policies on deforestation controls.

Appendix A

Table A1
Meteorological Stations and Data Series Information

Station	ANA Code	Station name	Latitude (deg)	Longitude (deg)	Times series	Duration (years)
1	655001	Km 1027 da BR-163	−75.1083	−55.2636	1983–2012	27
2	662001	Juma	−70.0833	−62.7872	1993–2012	17
3	755000	Novo Progresso	−70.6056	−55.4078	1998–2012	13
4	759000	Vila do Apui	−72.0444	−59.8931	1983–2012	30
5	760000	Prainha Velha	−72.0500	−60.6436	1975–2012	36
6	760001	Boca do Guariba	−77.0528	−60.5783	1978–2012	35
7	761002	Fazenda Água Azul	−78.2278	−61.2442	1991–2012	22
8	761003	Fazenda Bela Vista	−78.5333	−61.3339	2004–2011	8
9	762002	Maici-mirim	−76.3083	−62.6606	1994–2012	19
10	762003	Maici-grande	−78.0278	−62.3478	1999–2012	14
11	763001	Humaitá	−75.1528	−63.0286	1983–2009	19
12	764003	Cristo	−74.6500	−64.2433	1976–2012	25
13	765000	Cachoeira	−77.1556	−66.0583	1978–2012	31
14	765001	São Bento	−75.3056	−65.3500	1983–2012	23
15	851000	Fazenda Rio Dourado	−83.4639	−51.4428	2000–2012	10
16	855000	KM 947 BR-163	−81.8722	−55.1194	1978–2012	32
17	857000	Santa Rosa	−88.7028	−57.4164	1983–2012	25
18	861001	Bodocó	−84.8333	−61.5333	1998–2004	7
19	861002	Bonamigo	−80.0167	−61.7497	2005–2011	7
20	862000	Tabajara	−89.3222	−62.0556	1978–2012	31
21	863005	Sítio Vista Alegre	−80.9778	−63.6475	1983–2010	21
22	863008	Porto Velho	−87.4194	−63.9025	2002–2009	8
23	865000	Fazenda Sheffer	−83.3444	−65.7194	1983–2012	25
24	954001	Cachimbo	−98.1861	−54.8864	1985–2012	24
25	954002	Guaranta do Norte	−99.7556	−54.9042	2005–2012	6
26	956001	Jusante Foz Peixoto de Azevedo	−96.4333	−56.0186	1994–2012	23
27	956002	Paranaita	−96.9389	−56.4742	2000–2012	13
28	957001	Novo Planeta	−95.6639	−57.3947	1994–2012	22
29	957002	Nova Monte Verde	−99.7694	−57.4739	2001–2012	11
30	958002	Colniza	−94.5611	−58.2242	2001–2012	9
31	958004	Cotriguaçu	−99.1333	−58.5642	2005–2012	8
32	961003	Fábio (boliche)	−96.8139	−61.9789	1987–2012	23
33	962000	Mineração Oriente Novo	−95.8639	−62.3939	1979–2012	28
34	962001	Mineração Jacundá	−91.7917	−62.9531	1981–2006	23
35	963001	Santo Antônio BR-364	−92.6056	−63.1619	1978–2012	32
36	963004	Fazenda Rio Branco	−98.8722	−62.9878	1981–2011	29
37	963009	Ponte do Rio Preto do Crespo	−94.6667	−63.2500	1998–2011	13
38	964005	Jaciparaná	−92.5000	−64.4000	2004–2011	8
39	1052000	Vila São José do Xingu	−10.8072	−52.7461	1977–2012	31
40	1052001	Rio Comandante Fontoura	−10.5547	−52.1833	2000–2012	13
41	1052002	Jusante Rio Preto	−10.0472	−52.1144	2001–2012	11
42	1053001	Fazenda Santa Emília	−10.5392	−53.6089	1977–2012	27
43	1054000	Agropecuária Cajabi	−10.7461	−54.5461	1977–2012	27
44	1054002	Matupá	−10.1503	−54.9189	2005–2012	8
45	1055000	Estrada Cuiabá - Santarém	−10.2203	−54.9711	2004–2012	7
46	1055001	Indeco	−10.1125	−55.5700	1976–2012	30
47	1055003	Fazenda Tratex	−10.9542	−55.5486	1995–2012	17
48	1055004	Terra Nova do Norte	−10.6044	−55.1033	2001–2011	10
49	1056001	Estância Buriti	−10.3894	−56.4172	2001–2012	10
50	1057001	Trivelato	−99.4167	−57.1331	1983–2012	24
51	1058002	Núcleo Ariel	−98.5639	−58.2489	1983–2012	23
52	1058003	Juruena	−10.3125	−58.5017	1985–2009	22
53	1058004	Novo Tangara	−10.8342	−58.8033	1985–2012	20
54	1058005	Vale do Natal	−10.5886	−58.8678	1986–2012	21
55	1058006	Rio Arinos	−10.6397	−58.0039	2002–2012	10

Table A1
(continued)

Station	ANA Code	Station name	Latitude (deg)	Longitude (deg)	Times series	Duration (years)
56	1059000	Humboldt	−10.1753	−59.4517	1979–2012	34
57	1060001	Fazenda Muiraquita	−10.4344	−60.5572	2000–2011	12
58	1061001	Ji-Paraná	−10.8494	−61.9306	1976–1996	20
59	1061002	Fazenda castanhal	−10.3969	−61.0453	1983–2012	20
60	1061003	Rondominas (barrocas)	−10.5169	−62.0014	1987–2011	23
61	1062001	Jaru	−10.4458	−62.4656	1977–2011	31
62	1062002	Seringal 70	−10.2364	−62.6272	1979–2012	33
63	1062003	Mirante da serra	−11.0036	−62.6561	1984–2012	24
64	1062004	Theobroma	−10.2364	−62.3458	1987–2012	23
65	1063000	Escola Caramurú	−1.0505	−63.6461	1979–2012	28
66	1063002	Buritis	−10.2806	−63.7358	2011	1
67	1152001	Espigão	−11.3933	−52.2350	1985–2010	19
68	1154000	Rancho de Deus	−11.0028	−54.8053	1984–2011	22
69	1154001	Santa Felicidade	−11.9292	−54.9981	1983–2012	24
70	1154002	Fazenda Rio Negro	−11.5242	−54.3589	2000–2012	11
71	1154004	Claúdia	−11.4933	−54.8656	2005–2012	7
72	1154005	Riacho de Deus	−11.1272	−54.4767	2007–2012	6
73	1156001	Sinop (Fazenda Sempre Verde)	−11.6914	−55.4486	1984–2012	26
74	1156002	Tabaporã	−11.3047	−56.8250	2005–2012	7
75	1156003	Nova Americana	−11.6447	−56.1572	2005–2012	7
76	1157000	Porto dos Gaúchos	−11.5358	−57.4172	1974–2010	27
77	1157001	Juara	−11.2531	−57.5067	1984–2012	28
78	1157002	Olho d'água	−11.7150	−57.0419	2000–2012	12
79	1158002	Juína	−11.4081	−58.7186	1985–2012	26
80	1158003	Fazenda Tombador	−11.7178	−58.0472	1985–2012	24
81	1158004	Castanheira	−11.1400	−58.6161	2005–2012	6
82	1159000	Boteco dos mineiros	−11.8450	−59.3394	1985–2011	25
83	1160000	Marco Rondon	−12.0153	−6.0855	1978–2012	31
84	1161000	Vista Alegre	−11.4408	−61.4839	1978–2011	31
85	1161001	Pimenta Bueno	−11.6836	−61.1922	1980–2012	31
86	1161002	Rolim de Moura	−11.7497	−61.7764	1984–2012	25
87	1161003	Ministro Andreazza	−11.1969	−61.5281	1987–2002	27
88	1162003	São Miguel do Guaporé	−11.7325	−62.8025	2011–2012	2
89	1163000	São Francisco do Guaporé	−11.9664	−63.2722	2011–2012	2
90	1254001	Agrovensa	−12.8131	−54.7517	1983–2009	17
91	1254002	Consul	−12.3658	−54.4892	1998–2011	11
92	1254003	Agropecuária Três Irmãos	−12.7978	−54.2486	2001–2011	10
93	1255001	Teles Pires	−12.6750	−55.7931	1977–2012	24
94	1255002	Núcleo Colonial Rio Ferro	−12.5178	−54.9125	1977–2012	26
95	1256002	Fazenda Divisão	−12.9806	−56.3156	2000–2012	11
96	1257000	Brasnorte	−12.1164	−58.0003	1985–2012	26
97	1258001	Fazenda Floresta	−12.8675	−58.0703	2001–2012	7
98	1259001	Cachoeirinha	−12.0603	−59.6503	1985–2005	19
99	1260006	Chupinguaia	−12.5606	−60.9042	2007–2012	5
100	1261001	Parecis	−12.2092	−61.6286	2000–2012	13
101	1262001	Izidolândia	−12.6014	−62.1783	2000–2012	11
102	1354000	Fazenda Agrochapada	−13.4483	−54.2811	1983–2011	27
103	1354001	Agropecuária Malp	−13.3417	−54.0772	2000–2012	11
104	1354002	Fazenda Itaguaçu	−13.1381	−54.4439	2005–2011	7
105	1355001	Porto Roncador	−13.5564	−55.3317	1985–2008	22
106	1356004	São José do Rio Claro	−13.4450	−56.7275	2005–2012	7
107	1357000	Nova Maringá	−13.0661	−57.1133	1983–2012	25
108	1358002	Fazenda Tucunaré	−13.4667	−58.9750	1984–2012	27
109	1358003	Utiariti	−13.0333	−58.2833	1984–1986	3
110	1358007	Aldeia Sacre II	−13.0239	−58.1889	2005–2012	6
111	1359000	Padronal	−13.1831	−59.8769	1984–2012	27
112	1360000	Colorado do Oeste	−13.1142	−60.5483	1984–2011	27

Acknowledgments

This work was supported by CNPq, Brazil, processes 446412/2015-5 and 134400/2016-0. All the data used are archived at the Pangaea.de repository (https://doi.pangaea.de/10.1594/PANGAEA.893362).

References

Abrahão, G. M., & Costa, M. H. (2018). Evolution of rain and photoperiod limitations on the soybean growing season in Brazil: The rise (and possible fall) of double-cropping systems. *Agricultural and Forest Meteorology*, *256-257*, 32–45. https://doi.org/10.1016/j.agrformet.2018.02.031

Adekalu, K. O., Balogun, J. A., Aluko, O. B., Okunade, D. A., Gowing, J. W., & Faborode, M. O. (2009). Runoff water harvesting for dry spell mitigation for cowpea in the savannah belt of Nigeria. *Agricultural Water Management*, *96*(11), 1502–1508. https://doi.org/10.1016/j.agwat.2009.06.005

Assad, E., Sano, E., Masutomo, R., Hernan, R., De, C. L., & Macena, F. (1993). Veranicos na região dos Cerrados brasileiros frequência e probabilidade de ocorrência. *Pesquisa Agropecuária Brasileira*, *35*(6), 1159–1167. https://doi.org/10.1590/S0100-204X2000000600012

Assad, E. D., & Sano, E. E. (1998). *Sistema de informações geográficas—Aplicações na agricultura*, (2.ed. ed.p. 434). Brasília: EMBRAPA-CPAC.

Barron, J., & Okwach, G. (2005). Run-off water harvesting for dry spell mitigation in maize (*Zea mays* L.): Results from on-farm research in semi-arid Kenya. *Agricultural Water Management*, *74*(1), 1–21. https://doi.org/10.1016/j.agwat.2004.11.002

Barron, J., Rockström, J., Gichuki, F., & Hatibu, N. (2003). Dry spell analysis and maize yields for two semi-arid locations in east Africa. *Agricultural and Forest Meteorology*, *117*(1-2), 2327. https://doi.org/10.1016/S0168-1923(03)00037-6

Butt, N., de Oliveira, P. A., & Costa, M. H. (2011). Evidence that deforestation affects the onset of the rainy season in Rondonia, Brazil. *Journal of Geophysical Research*, *116*, D11120. https://doi.org/10.1029/2010JD015174

Carvalho, D. F., Faria, R. A., Sousa, S. A. V., & Borges, H. Q. (2000). Espacialização do período de veranico para diferentes níveis de perda de produção na cultura do milho, na bacia do Rio Verde Grande, MG. *Revista Brasileira de Engenharia Agrícola e Ambiental*, *4*(2), 172–176. https://doi.org/10.1590/S1415-43662000000200007

Carvalho, G., Barros, A. C., Moutinho, P., & Nepstad, D. (2001). Sensitive development could protect Amazonia instead of destroying it. *Nature*, *409*(6817), 131. https://doi.org/10.1038/35051794

Ceballos, A., Mertínez-Fernández, J., & Luego-Ugidos, M. A. (2004). Analysis of rainfall trends and dry periods on a pluviometric gradient representative of Mediterranean climate in the Duero Basin, Spain. *Journal of Arid Environments*, *58*(2), 215–233. https://doi.org/10.1016/j.jaridenv.2003.07.002

Chambers, J. Q., & Artaxo, P. (2017). Deforestation size influences rainfall. *Nature Climate Change*, *7*(3), 175–176. https://doi.org/10.1038/nclimate3238

Costa, M. H., & Foley, J. A. (1997). Water balance of the Amazon Basin: Dependence on vegetation cover and canopy conductance. *Journal of Geophysical Research*, *102*(D20), 23,973–23,989. https://doi.org/10.1029/97JD01865

Costa, M. H., & Pires, G. (2010). Effects of Amazon and Central Brazil deforestation scenarios on the duration of the dry season in the arc of deforestation. *International Journal of Climatology*, *30*, 1970–1979. https://doi.org/10.1002/joc.2048

Culf, A. D., Esteves, J. L., Marques Filho, A., de, O., & da Rocha, H. R. (1996). Radiation, temperature and humidity over forest and pasture in Amazonia. In J. H. C. Gash, et al. (Eds.), *Amazonian Deforestation and Climate* (pp. 175–191). New York: John Wiley.

Davidson, E., de Araújo, A., Artaxo, P., Balch, J., Brown, F., Bustamante, M., et al. (2012). The Amazon basin in transition. *Nature*, *481*(7381), 321–328. https://doi.org/10.1038/nature10717

Debortoli, N. S., Dubreuil, V., Funatsu, B., Delahaye, F., de Oliveira, C. H., Rodrigues-Filho, S., et al. (2015). Rainfall patterns in the southern Amazon: A chronological perspective (1971–2010). *Climate Change*, *132*(2), 251–264. https://doi.org/10.1007/s10584-015-1415-1

Debortoli, N. S., Dubreuil, V., Hirota, M., Rodrigues Filho, S., Lindosoa, D. P., & Nabucetb, J. (2016). Detecting deforestation impacts in Southern Amazonia rainfall using rain gauges. *International Journal of Climatology*, *37*(6), 2889–2900. https://doi.org/10.1002/joc.4886

Dias, L. C. P., Pimenta, F. M., Santos, A. B., Costa, M. H., & Ladle, R. J. (2016). Patterns of land use, extensification and intensification of Brazilian agriculture. *Global Change Biology*, *22*(8), 2887–2903. https://doi.org/10.1111/gcb.13314

Doorenbos, J., & Kassam, A. H. (1979). Yield response to water. FAO Irrigation and Drainage Paper,33. Rome, FAO.

Dubreuil, V., Merot, P., Delahaye, D., & Desnos, P. (2012). Changement climatique dans l'Ouest. Rennes, Presses Universitaires de Rennes, 464.

Erfanian, A., Wang, G., & Fomenko, L. (2017). Unprecedented drought over tropical South America in 2016: Significantly under-predicted by tropical SST. *Scientific Reports*, *7*(1), 5811. https://doi.org/10.1038/s41598-017-05373-2

Espinoza, W., Azevedo, J., & Rocha, L. D. (1980). Densidade de plantio e irrigação suplementar na resposta de três variedades de milho ao déficit hídrico na região de cerrados. *Pesquisa Agropecuária Brasileira*, *15*, 85–95.

Espinoza, W., Azevedo, L. G. & Jarreta Júnior, M. (1982). O clima da região dos Cerrados em relação à agricultura. Planaltina., DF: EMBRAPACPAC, 37. (EMBRAPA-CPAC. Circular técnica, 9).

Ferreira, V. L., Venticinque, E., & Almeida, S. (2005). O desmatamento na Amazônia e a importância das áreas protegidas. *Estudos Avançados*, *19*(53), 157–166. https://doi.org/10.1590/S0103-40142005000100010

Fetter, R., de Oliveira, C. H., & Steinke, E. T. (2018). Um Índice para Avaliação da Variabilidade Espaço-Temporal das Chuvas no Brasil. *Revista Brasileira de Meteorologia*, *33*(2), 225–237. https://doi.org/10.1590/0102-7786332002

Figueroa, S. N., & Nobre, C. A. (1990). Precipitation distribution over central and western tropical South America. *Climanálise*, *5*, 36–45.

Fox, P., & Rockström, J. (2003). Supplemental irrigation for dry-spell mitigation of rainfed agriculture in the Sahel. *Agricultural Water Management*, *61*(1), 29–50. https://doi.org/10.1016/S0378-3774(03)00008-8

Fu, R., Yina, L., Wenhong, L., Ariasc, P. A., Dickinson, R. E., Huanga, L., et al. (2013). Increased dry-season length over southern Amazonia in recent decades and its implication for future climate projection. *Proceedings of the National Academy of Sciences*, *110*(45), 18,110–18,115. https://doi.org/10.1073/pnas.1302584110

Fu, R., Zhu, B., & Dickinson, E. (1999). How do atmosphere and land surface influence seasonal changes of convection in the tropical amazon? *Journal of Climate*, *12*(5), 1306–1321. https://doi.org/10.1175/1520-0442(1999)012<1306:HDAALS>2.0.CO;2

Gan, M. A., Kousky, V. E., & Ropelewski, C. F. (2004). The South American monsoon circulation and its relationship to rainfall over west-central Brazil. *Journal of Climate*, *17*(1), 47–66. https://doi.org/10.1175/1520-0442(2004)017<0047:TSAMCA>2.0.CO;2

Gash, J. H. C., & Nobre, C. A. (1997). Climatic effects of Amazonian deforestation: Some results from ABRACOS. *Bulletin of the American Meteorological Society*, *78*(5), 823–830. https://doi.org/10.1175/15200477(1997)078<0823:CEOADS>2.0.CO;2

Hansen, M. C., Potapov, P. V., Moore, R., Hancher, M., Turubanova, S. A., Tyukavina, A., et al. (2013). High-resolution global maps of 21st-century forest cover change. *Science*, *342*(6160), 850–853. https://doi.org/10.1126/science.1244693

Hernandez, F. B. T., Souza, S. A. V., De Zocoler, J. L., & Frizzone, J. A. (2003). Simulação e efeito de veranicos em culturas desenvolvidas na região de Palmeira d'Oeste, Estado de São Paulo. *Engenharia Agrícola*, *23*, 21–30.

Instituto Nacional De Pesquisas Espaciais (2012). Monitoramento da Floresta Amazônica Brasileira por Satélite: 2012. (Online) http://www.obt.inpe.br/prodes.

Khanna, J., & Medvigy, D. (2014). Strong control of surface roughness variations on the simulated dry season regional atmospheric response to contemporary deforestation in Rondônia, Brazil. *Journal of Geophysical Research: Atmospheres*, *119*, 13,067–13,078. https://doi.org/10.1002/2014JD022278

Khanna, J., Medvigy, D., Fueglistaler, S., & Walko, R. (2017). Regional dry-season climate changes due to three decades of Amazonian deforestation. *Nature Climate Change*, *7*(3), 200–204. https://doi.org/10.1038/NCLIMATE3226

Laurance, W. F., Cochrane, M. A., Bergen, S., Fearnside, P. M., Delamônica, P., Barber, C., et al. (2001). The future of Brazilian Amazon. *Science*, *291*(5503), 438–439. https://doi.org/10.1126/science.291.5503.438

Liebmann, B., Camargo, S. J., Seth, A., Marengo, J. A., Carvalho, L. M. V., Allured, D., et al. (2007). Onset and end of the rainy season in South America in observations and the ECHAM 4.5 atmospheric general circulation model. *Journal of Climate*, *20*(10), 2037–2050. http://doi.org/10.1175/JCLI4122

Liebmann, B., & Mechoso, C. R. (2011). The South American monsoon system. In C.-P. Chang et al. (Ed.), *The Global Monsoon System: Research and Forecast*, (2nd ed. pp. 137–157). Singapore: World Scientific. ISBN 9814343412, 9789814343411.

Macedo, N. M., DeFries, R. S., Morton, D. C., Stickler, C. M., Galford, G. L., & Shimabukuro, Y. E. (2012). Decoupling of deforestation and soy production in the southern Amazon during the late 2000s. *PNAS*, *109*, 13411346. https://doi.org/10.1073/pnas.1111374109

Marengo, J. (1995a). Interannual variability of deep convection in the tropical South American sector as deduced from ISCCP C2 data. *International Journal of Climatology*, *15*(9), 9951010. https://doi.org/10.1002/joc.3370150906

Marengo, J. (1995b). Variations and change in South American streamflow. *Climate Change*, *31*(1), 99–117. https://doi.org/10.1007/BF01092983

Marengo, J. (2004). Interdecadal variability and trends of rainfall across the Amazon basin. *Theoretical and Applied Climatology*, *78*(1-3), 79–96. https://doi.org/10.1007/s00704-004-0045-8

Marengo, J. A., Liebmann, B., Kousky, V. E., Filizola, N. P., & Wainer, I. C. (2001). Onset and end of the rainy season in the Brazilian Amazon basin. *Journal of Climate*, *14*(5), 833–852. https://doi.org/10.1175/1520-0442(2001)014<0833:OAEOTR>2.0.CO;2

McHugh, O. V., Steenhuis, T. S., Abebe, B., & Fernandes, E. C. M. (2007). Performance of in situ rainwater conservation tillage techniques on dry spell mitigation and erosion control in the drought-prone North Wello zone of the Ethiopian highlands. *Soil & Tillage Research*, *97*(1), 19–36. https://doi.org/10.1016/j.still.2007.08.002

Minuzzi, R. B., Sediyama, G. C., Ribeiro, A., & Costa, J. M. N. (2005). El Niño: ocorrência e duração dos veranicos do Estado de Minas Gerais. *Revista Brasileira de Engenharia Agrícola e Ambiental*, *9*(3), 364–371. https://doi.org/10.1590/S1415-43662005000300011

Morton, D. C., DeFries, S. R., Shimabukuro, E. Y., Anderson, L., Arai, E., del Bon Espirito-Santo, F., et al. (2006). Cropland expansion changes deforestation dynamics in the southern Brazilian Amazon. *Proceedings of the National Academy of Sciences*, *103*(39), 14,637–14,641. https://doi.org/10.1073/pnas.0606377103

Nepstad, D., Carvalho, G., Barros, A. C., Alencar, A., Capobianco, J. B., Bishop, J., et al. (2001). Road paving, fire regime feedbacks, and the future of Amazon forests. *Forest Ecology and Management*, *154*(3), 395–407. https://doi.org/10.1016/S0378-1127(01)00511-4

Odekunle, T. O., & Buyiro, S. O. G. (2003). Rain days predictability in southwestern Nigeria. *Journal of Nigerian Meteorological Society*, *4*, 1–17.

Oliveira, A. D. (2000). *Aspectos agroclimáticos do arroz de sequeiro no estado de Minas Gerais*, (p. 56). Viçosa, MG: UFV.

Pebesma, E., & Heuvelink, G. (2016). Spatio-temporal interpolation using gstat. *RFID Journal*, *8*, 204–218.

Pebesma, E. J. (2004). Multivariable geostatistics in S: The gstat package. *Computers and Geosciences*, *30*(7), 683–691. https://doi.org/10.1016/j.cageo.2004.03.012

Schubert, S. D., Suarez, M. J., Pegion, P. J., Randal, D. K., & Bacmeister, J. T. (2004). Causes of long-term drought in the United States Great Plains. *Journal of Climate*, *17*(3), 485–503. https://doi.org/10.1175/1520-0442(2004)017<0485:COLDIT>2.0.CO;2

Shapiro, S. S., & Wilk, M. B. (1965). An analysis of variance test for normality (complete samples). *Biometrika*, *52*(3-4), 591–611. https://doi.org/10.1093/biomet/52.3-4.591

Sharma, T. C. (1996). Simulation of the Kenyan longest dry and wet spells and the largest rain-sums using a Markov model. *Journal of Hydrology*, *178*(1-4), 55–67. https://doi.org/10.1016/0022-1694(95)02827-7

Silva, F. A. S., & Rao, T. V. R. (2002). Regimes pluviais, estação chuvosa e probabilidade de ocorrência de veranicos no estado do Ceará. *Revista Brasileira de Engenharia Agrícola e Ambiental*, *6*(3), 440–446. https://doi.org/10.1590/S1415-43662002000300010

Sleiman, J. (2008). Veranicos ocorridos na porção noroeste do estado do rio Grande do Sul entre 1978 e 2005 e sua associação às condições climáticas na atmosfera. Dissertação de Mestrado, Universidade de São Paulo, Departamento de Geografia, São Paulo, SP, 164.

Soares, D. B., & Nóbrega, R. S. (2010). Análise espacial e climatológica da ocorrência de veranicos no sertão de Pernambuco. *Revista de Geografia*, *27*, 95–106.

Sombroek, W. (2001). Spatial and temporal patterns of Amazon rainfall. *Ambio*, *30*, 388396. https://doi.org/10.1579/0044-7447-0.7.388

Spangler, K. R., Lynch, A. H., & Spera, S. A. (2017). Precipitation drivers of cropping frequency in the Brazilian cerrado: Evidence and implications for decision-making. *Weather, Climate, and Society*, *9*(2), 201–213. https://doi.org/10.1175/WCAS-D-16-0024.1

Stern, R. D., & Coe, R. (1982). The use of rainfall models in agricultural planning. *Agricultural Meteorology*, *26*(1), 35–50. https://doi.org/10.1016/0002-1571(82)90056-5

Sugahara, S. (1991). Flutuações interanuais, sazonais e inatrasazonais da precipitação no estado de São Paulo. Ph.D. thesis, Universidade de São Paulo, 140.

Wright, J., Fu, R., Fu, R., John, W. R., Chakraborty, S., Clinton, N. E., et al. (2017). Rainforest-initiated wet season onset over the southern Amazon. *Proceedings of the National Academy of Sciences*, *114*(32), 8481–8486. https://doi.org/10.1073/pnas.1621516114